

Energy & Environmental Science

Accepted Manuscript



This is an *Accepted Manuscript*, which has been through the Royal Society of Chemistry peer review process and has been accepted for publication.

Accepted Manuscripts are published online shortly after acceptance, before technical editing, formatting and proof reading. Using this free service, authors can make their results available to the community, in citable form, before we publish the edited article. We will replace this *Accepted Manuscript* with the edited and formatted *Advance Article* as soon as it is available.

You can find more information about *Accepted Manuscripts* in the [Information for Authors](#).

Please note that technical editing may introduce minor changes to the text and/or graphics, which may alter content. The journal's standard [Terms & Conditions](#) and the [Ethical guidelines](#) still apply. In no event shall the Royal Society of Chemistry be held responsible for any errors or omissions in this *Accepted Manuscript* or any consequences arising from the use of any information it contains.

Trapping lithium polysulfides of a Li-S battery by forming lithium bonds in a polymer matrix

Kyusung Park¹, Joon Hee Cho², Ji-Hoon Jang¹, Byeong-Chul Yu¹, Andrea T. De La Hoz³, Kevin M. Miller³, Christopher J. Ellison^{1,2}, and John B. Goodenough^{1*}

¹Texas Materials Institute and ²McKetta Department of Chemical Engineering, The University of Texas at Austin, Austin, TX 78712, United States

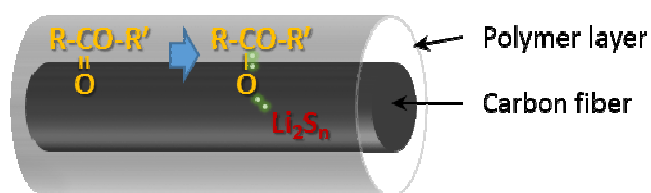
³Department of Chemistry, Murray State University, Murray, KY 42071, United States

*Corresponding author. E-mail: jgoodenough@mail.utexas.edu

Abstract

Despite great interests in a Li-S battery, soluble polysulfides as charge/discharge intermediates pose an important challenge to realize commercial Li-S batteries. From building physical barriers to reduce a diffusional loss of those species, chemical surface-trap-sites have been proposed, but experimental evidences about the trapping interaction haven't been reported. Here, highly crosslinked polymer-electrolyte coating layers with electron-donating groups were designed to bind the lithium polysulfides. An ester group with a high spatial density was shown to be a strong candidate to bind the lithium polysulfides. Spectroscopic evidences for the presence of lithium bonds between the lithium polysulfides and the electron-donating groups are reported for the first time. An electrochemical charge/discharge model is also proposed that can explain the electrochemical behavior within the insulating polymer layer.

Table of contents entry



Trapping lithium polysulfides of a Li-S battery has been successfully demonstrated by forming lithium bonds in a polymer matrix.

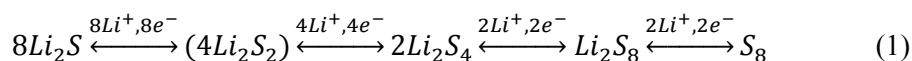
Lithium-sulfur batteries have been extensively studied as a high-capacity alternative to lithium-ion batteries.¹⁻³ The electrochemical reactions of sulfur involve several intermediates, lithium polysulfides (Li_2S_n , $4 \leq n \leq 8$) that are soluble in the liquid electrolyte, which induces a continuous loss of active material from a sulfur cathode. To overcome this problem, most research efforts have focused on confining sulfur with sophisticated high-surface-area carbon nanostructures. However, since the liquid electrolyte must be connected to all the pore structures to utilize full capacity, the soluble polysulfides are always exposed and prone to diffuse into the electrolyte and to the anode. Several reports regarding trapping of the soluble species by chemical interactions with the cathode surface have been published recently, but this approach is still limited by the surface density of the interactive sites compared to the amount of dissolved species in the bulk liquid electrolyte.⁴⁻¹⁰ In this paper, we show a polymer layer with electron-donating functional groups that can provide effective binding sites for lithium polysulfides; and the binding performance doesn't depend on surface area, but on the bulk density of the electron donating groups. The strategy of this approach is not only to limit outbound diffusion of the soluble Li_2S_n molecules, but also to capture the soluble species close to one another to facilitate, on recharge, the reformation of S_8 molecules.

Highly cross-linked polymers with various functional groups were prepared via thiol-ene chemistry.^{11,12} A tetrathiol crosslinker (pentaerythritol tetrakis (3-mercaptopropionate), *PETT*) was polymerized with four different kinds of difunctional ene monomers with unique functional groups, 1,6-divinylperfluorohexane (*FC*), di(ethylene glycol) divinyl ether (*EO*), divinyl adipate (*Ester*), and 1,6-bis(vinylsulfone)hexane (*Sulfone*) as listed in Fig. 1a. They were made as neat membranes for analysis and coated onto sulfur-loaded carbon papers for electrochemical tests as shown in Fig. 1b; they are referred to hereafter as PETT-FC, PETT-EO, PETT-Ester, and PETT-Sulfone, respectively. The polymers have similar molecular mesh sizes between crosslink junction points ranging from 27.1 to 30.5 Å (See Supplementary Information.). With ATR-FTIR analysis, we confirmed successful formation of these polymers along with complete conversion of the precursor monomers following thiol-ene polymerization as shown in Fig. 1c (See Supplementary Information for a detailed discussion.).

The polymers have distinctive glass transition temperatures as listed in Table 1 (See Supplementary Information). The PETT-EO and PETT-Ester thiol-ene networks exhibit T_g s at $-30.9\text{ }^\circ\text{C}$ and $-19.9\text{ }^\circ\text{C}$, respectively, while PETT-FC showed a T_g at $6.3\text{ }^\circ\text{C}$. On the other hand, the T_g of PETT-Sulfone was at $30.8\text{ }^\circ\text{C}$, which is above room temperature. The polymer membranes were soaked in a 1:1 volume mixture of dimethoxyethane and dioxolane (DME/DOL) at room temperature, and their weights were monitored with time as shown in Fig. 2a. All of the membranes showed very fast swelling and were stable in the electrolyte solvent more than 1 week. PETT-Sulfone showed the lowest degree of swelling ($\sim 19\%$) probably because its T_g is above room temperature. PETT-FC showed the highest swelling ability ($\sim 79\%$), while PETT-EO ($\sim 57\%$) and PETT-Ester ($\sim 52\%$) showed moderate swelling values. The equilibrium amount of electrolyte uptake is a function of the crosslink density and affinity of the electrolyte for the polymer. It is worth noting that the polymers reported here swell significantly less than those of typical gel-polymer electrolytes¹³, which is most likely owing to the high cross-linking density in our polymers. We believe the low degree of swelling and the chemical stability in the electrolyte are important to limit diffusional loss of the polysulfides to the electrolyte and to maximize chemical interactions between polymers and lithium polysulfides. Moreover, it is well-known that the cell performance of a Li-S cell strongly depends on the amount of the liquid electrolyte,^{14,15} but in our polymer-coated electrodes, the amount of electrolyte is solely controlled by the uptake characteristics of the polymer component, and hence doesn't need to be further optimized.

Figs. 2b and c show battery-cell performances of the bare sulfur-loaded carbon-paper electrode, PETT-FC, PETT-EO, PETT-Ester, and PETT-Sulfone. The bare electrode showed a poor initial coulombic efficiency of 75.5% and cycled up to only 28 cycles before the cell was terminated by the endless polysulfide shuttle current. The low cycling capacity indicates that a large amount of active sulfur was lost in the liquid electrolyte during either the electrode soaking in the liquid electrolyte or the cell operation since the carbon paper doesn't provide any geometric structures to hold the soluble polysulfide species.¹⁶ Thin polymer layers on the carbon paper don't seem to impede the electronic conduction between the trapped polysulfides and the carbon as displayed in Fig. 2c, which is in agreement with a previous report on a polyethylene-glycol-encapsulated

sulfur/carbon cathode.¹⁷ We speculate how that occurs at the end of this paper. PETT-FC also exhibits similar capacities to those of the bare electrode, but the cycle stability lasts up to 200 cycles. We speculate that the poor performance of PETT-FC is owing to the highest degree of swelling; too large an amount of liquid electrolyte is present in the polymer coating layer and is connected to the bulk electrolyte. Moreover, some active sulfur diffusion out of the polymer coating layer during the soaking process could reduce coulombic efficiencies during cycling. Nevertheless, by the second cycle, the discharge curve shows the characteristic two voltage regions of a sulfur cathode; the initial voltage region at 2.4 ~ 2.1 V corresponds to the reaction of S₈ or Li₂S₈ to Li₂S₄, the second plateau at 2 V makes the reduction of Li₂S₄ to Li₂S via Li₂S₂. On recharge, it is necessary to reconstitute S₈ from Li₂S by removal of Li⁺ and e⁻ as represented in equation (1). Li₂S₆ is also present via a partial disproportionation of Li₂S₈, but it is not included in this equation for simplicity. This process requires the interaction of 8Li₂S to make S₈.



However, Li₂S_n (4 ≤ n ≤ 8) species are soluble in an organic liquid electrolyte; unless they are trapped long enough on discharge to be reduced to insoluble Li₂S₂/Li₂S before they migrate from their reaction sites, the soluble species carry sulfur away from the original cathode. Owing to the solubility limit of the electrolyte, the soluble species are deposited on some surface in the cell, but unless the surface makes electronic contact with the cathode, no further oxidation occurs. Li₂S₄ is soluble in the liquid electrolyte, but it is not soluble as much as Li₂S₆ and Li₂S₈.¹⁸ On the other hand, it may be oxidized at a site far removed initially from other sulfur species, which would limit, on charge, its oxidation beyond Li₂S₄. It follows that a strategy for a sulfur cathode would need to include (1) an electrolyte with as small a solubility limit as possible and (2) a large concentration of sites that trap the soluble species and are accessible to electrons from the cathode.

In contrast to PETT-FC, PETT-Sulfone with the lowest degree of swelling shows even lower initial capacities with a unique cycling performance. Note that there is initially no 2 V voltage plateau that corresponds to the formation of solid Li₂S₂ and Li₂S; this plateau appears slowly in the later cycles. Because (1) PETT-

Sulfone is stiff at room temperature (See Table 1) and (2) Li_2S (1.66 g cm^{-3}) needs more space to grow than is occupied by S_8 (2.03 g cm^{-3}),² it appears to be dimensionally unfavorable to form $8\text{Li}_2\text{S}$ in between PETT-Sulfone and the carbon fibers where sulfur resides before cycling. As the lower voltage plateau appears, the cycling capacities were increased, but they were saturated at $\sim 550 \text{ mAh g}^{-1}$. Repeated formation and dissolution cycles of sulfur must have induced removal of some active material, which caused a cell termination by an endless shuttle current in the 161st cycle.

PETT-EO and PETT-Ester show a significant increases in the reversible capacities: the initial discharge capacities are 1260 and 1018 mAh g^{-1} , respectively, with the two distinct voltage regions at 2.4 and 2.0 V. The initial discharge polarization disappeared already by the second cycle with PETT-EO, but capacities continuously decrease during the initial 10 cycles. The loss mainly happens in the lower voltage region, which is associated with the diffusional loss of the soluble active materials. With PETT-Ester, on the other hand, the discharge polarization did not quickly disappear as in PETT-EO and the capacities were remarkably stable throughout the cycle test. This observation signals that the ester group is a more efficient trap of the soluble Li_2S_4 .

To probe any chemical interactions between polymer backbones and lithium polysulfides, specifically Li_2S , the product of a reduced trapped polysulfides, discharged cells were prepared for XPS and FTIR analyses. We didn't test PETT-Sulfone because it doesn't form Li_2S in the initial cycles as shown in Fig. 2c. Fig. 3a shows measured and fitted Li 1s XPS spectra. The bare sulfur/carbon electrode without a polymer coating has an additional peak component at 53.69 eV that can be assigned to Li_2O , an electrolyte decomposition product.¹⁹ The polymer coating remarkably enhances electrolyte stability and only brings a single peak associated with Li_2S .^{19,20} Here we found that the Li 1s XPS peaks of Li_2S in the bare, PETT-FC, PETT-EO and PETT-Ester electrodes were shifted progressively to lower values from 55.19 to 54.95, 54.65, and 54.40 eV, respectively. The lithium in Li_2S is partially reduced in the presence of the polymer layer. To find the corresponding electron donating component, FTIR spectra were analyzed with the same electrode samples as shown in Fig. 3b. The COO stretch vibration shows red shifts from 1425.16 to 1421.3, 1419.37, and 1419.37 cm^{-1} while the CO vibration exhibits

blue shifts from 989.32 to 995.1, 995.1, and 997.03 cm^{-1} in the bare, PETT-FC, PETT-EO and PETT-Ester electrodes, respectively.²⁰ The results clearly indicate that the carbonyl double bond in the ester group releases electronic charge to lithium in the lithium polysulfides to form an asymmetric lithium bond as illustrated in Fig. 3, which induces the red shifts in the COO vibration and blue shifts in the CO vibration.^{21,22} At the atomic level, pure sulfur S_8 molecules should interact via van der Waals attraction, but after lithiation of the terminated sulfurs in Li_2S_n ($4 \leq n \leq 8$), electrostatic interactions between lithium and sulfur or asymmetric bonding by a covalent component between lithium and surrounding chemical environments become more important. This is the first experimental evidence for forming a lithium bond between Li_2S_n and a host electron-donor site. Our results strongly suggest that forming lithium bonds with functional groups in the polymer backbone that are strong enough to overcome the dissolution interaction of the lithium polysulfides is important to reduce the diffusional loss of the active materials to the liquid electrolyte.

Moreover, it is worth noting that the degree of the shifts in XPS and FTIR signals is a function of spatial density of the ester group: the denser the ester groups, the greater the shifts. For example, PETT-FC and PETT-EO have the same number of ester groups in the structure as is illustrated in Fig. 1b, but PETT-FC uptakes more electrolyte and therefore has a lower ester density in the presence of the liquid electrolyte. PETT-Ester has the highest ester density of the polymer structures (Fig. 1b), and the degree of swelling is also lower than that of PETT-EO. The ester group is a stronger electron donating group than ethylene oxide and is, therefore, more effective to bind lithium species according to our results.²³ Unlike previous reports demonstrating effective surface sites to trap lithium polysulfides^{4-7,24}, ester groups present in the bulk of the polymer layer provide stronger and/or a lot more binding sites for lithium polysulfides. There are four ester groups between crosslinkers (4 per 29.6 Å) in PETT-Ester (Fig. 1b), and the functional group arrays are three dimensionally present. The more binding sites and the stronger binding force in PETT-Ester result in a more stable cycle life without the initial capacity loss that was seen in the PETT-EO electrode.

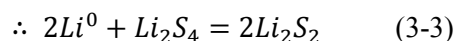
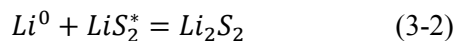
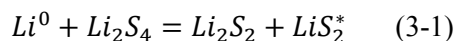
Finally, the lithium bonding to the polymer should also affect the rechargeability of the lithium polysulfides. The initial recharge step to oxidize $\text{Li}_2\text{S}_2/\text{Li}_2\text{S}$ to the soluble Li_2S_4 is kinetically limited because it

involves a solid reconstitution reaction. However, it can be promoted by the presence of soluble polysulfides or sulfur radicals that can, on charge, chemically attack surface radicals of Li-deficient $\text{Li}_2\text{S}_2/\text{Li}_2\text{S}$ to take Li_2S_n ($4 \leq n \leq 6$) into solution as described in detail in the following section.^{18,25} Since the ester groups provide binding sites for the lithium polysulfides, the proximity of the insoluble products $\text{Li}_2\text{S}_2/\text{Li}_2\text{S}$ to one another on neighboring trap sites can facilitate the slow oxidation reaction to Li_2S_4 . To avoid capacity fading, this step requires a relatively fast transport of Li_2S_4 species either through the liquid electrolyte or over the polymer surface before loss of Li_2S_4 to an adsorption site far from another Li_2S_4 molecule. The final step of the Li_2S_8 oxidation to S_8 as represented in equation (1) is accomplished by only removal of electrons and 2Li^+ for reconfiguration of the molecule in place. This sequence depends on having (1) the trapped polysulfides on the polymer not too far removed from a carbon fiber for electron tunneling and (2) the polysulfides not so tightly trapped that the soluble species can move to react with one another to form Li_2S_8 and S_8 . These requirements mean that the polymer films in this work can be expected to have an optimal thickness and not too strong a trapping Li bond with a high concentration of trapping sites.

The reduction/oxidation reactions of the sulfur species require the transfer of electrons between the cathode and the sulfur species. Where the sulfur is located on the carbon paper in the initial reduction reaction, electron transfer to the sulfur from the metallic cathode via surface Li^0 atoms to reduce S_8 to Li_2S_8 does not pose a conceptual problem. However, once the Li_2S_8 is attacked to create soluble Li_2S_6 and Li_2S_4 that become trapped partly at an insulating polymer ester group removed from the carbon paper, further reduction to $\text{Li}_2\text{S}_2/\text{Li}_2\text{S}$ requires electron transfer through the electrolyte. Unless electron tunneling within a limited distance from the carbon fiber surface is allowed, this transfer would require a soluble carrier molecule or atom. We suggest that electrons, once transferred to a surface Li^+ ion that is removed from sulfur, are repelled from the negative charge on the cathode and move as Li^0 via Li^+ ions that are attracted to the cathode surface. The electron transfer as a Li^0 would be terminated by its reaction with a reducible sulfur species in, for example,

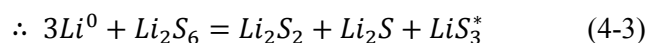
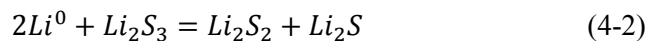
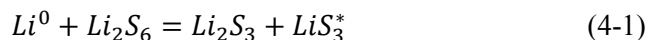


For n=2:



The reactive LiS_2^* would react with another Li^0 to form a second insoluble Li_2S_2 as described in equation (3-2), but LiS_2^* hasn't been detected in a Li-S cell.

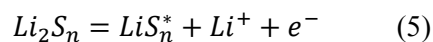
For n=3:



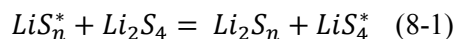
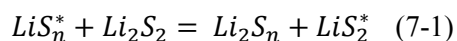
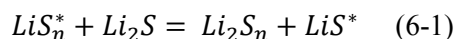
LiS_3^* reportedly forms by direct dissociation of Li_2S_6 , but it can also be generated as described in equation (4-1). LiS_3^* is present during charge/discharge according to *in-situ* spectroscopy studies, and its concentration becomes maximum right before the 2 V plateau begins.^{18,26–28} The dissociation of Li_2S_6 alone cannot explain the concentration variation that makes equation (4-1) feasible. However, Li_2S_3 ($=2Li^+ + S_3^{2-}$) has been reported only in an *ex-situ* observation after rinsing electrode samples in a Li^+ -free organic solvent.²⁹ Therefore, it is likely that the center sulfur atom in the S_3 chain of metastable Li_2S_3 reacts with $2Li^0$ to form Li_2S_2 and Li_2S during discharge as in equation (4-2). Direct reduction of LiS_3^* to Li_2S_3 is also possible, which will undergo a subsequent reaction like equation (4-2). The overall reaction can be written as equation (4-3), and this reaction scheme is also valid in the case of direct electron tunneling from the carbon surface.

Although this scheme is plausible for the reduction reaction, another process is needed for the oxidation recharge reaction. For the oxidation reaction, we consider the observation that oxidation is greatly enhanced by

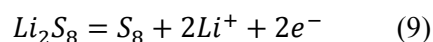
the presence of soluble molecules Li_2S_n ($4 \leq n \leq 8$).²⁵ At the carbon-paper surface on charge, a soluble Li_2S_n molecule would be oxidized by the reaction



to create a soluble electron-hole carrier, LiS_n^* . We believe that this hole carrier reacts with Li_2S_n as follows.



The soluble Li_2S_8 is oxidized at the carbon-paper cathode:



In summary, we have shown a new way, without using sophisticated nanostructures, to bind the soluble lithium polysulfides with polymer coating layers functionalized with electron donating groups. Ester groups on a polymer backbone form lithium bonds with the lithium polysulfides, which brings a significant capacity increase and enhances charge/discharge cycle stability compared to the bare sulfur/carbon electrode. Electron-donating ability and spatial density of the functional group are important factors to control the strength of the Li-polymer interactions and the corresponding electrochemical performances. Highly cross-linked thiol-ene polymers are effective in this regard. Lastly, it should be noted that the presence of electron-donating functional groups can hinder Li^+ transport, so it is important to choose the proper electron donating group that is not too strong to hamper Li^+ diffusion and not too weak to trap the lithium polysulfides.

Experimental section

Materials for polymerization. Pentaerythritol tetrakis (3-mercaptopropionate) (PETT, $M_n = 489 \text{ g mol}^{-1}$; Sigma Aldrich) was used as a crosslinker, and Irgacure 2100 (BASF) was used as a photoinitiator during thiol-ene polymerization reactions. Three monomers were purchased and used as received: di(ethylene glycol) divinyl ether ($M_n = 158 \text{ g mol}^{-1}$; BASF), divinyl adipate ($M_n = 198.22 \text{ g mol}^{-1}$; Polysciences, Inc.), and 1,6-divinylperfluorohexane ($M_n = 354.14 \text{ g mol}^{-1}$; Matrix scientific). The 1,6-bis(vinylsulfone)hexane ($M_n = 266.38 \text{ g mol}^{-1}$) was prepared as described in the Supplementary Information.³⁰

Polymerization and electrode preparation. For the polymer coating on the carbon-paper electrodes, four different monomer solutions were prepared: 0.1 g of PETT was mixed with each monomer in 1 : 1 thiol-ene molar ratio and 3 wt.% of a photoinitiator was added to the solution. The blend solutions, except the divinyl sulfone monomer, were further diluted with 1 mL tetrahydrofuran (THF) to make an appropriate concentration and viscosity for coating (a crosslinker concentration of $\sim 2 \text{ mol L}^{-1}$). The sulfone monomer solution was also prepared with the same ratio, but chloroform was used as a solvent owing to a solubility limit of the monomer powder. All these mixing procedures were carried out in a UV light free room to minimize the thiol-ene reaction. The same procedure was also used to make neat polymer membranes for DSC and electrolyte soaking tests.

Commercially available carbon paper (SIGRACET GDL 10 BA, Ion Power, Inc.) was used for electrode preparation. It had a thickness of 400 μm and a porosity of 88 %. Sulfur was loaded onto the carbon paper by drop coating with sulfur-dissolved carbon disulfide solution. The coated carbon paper was further heat treated at 155 °C for 20 hours to promote homogeneous coating. The resulting carbon paper was punched into 3/8-inch discs and used for subsequent polymer coating by the thiol-ene chemistry. Sulfur loading of the carbon disc ranged within 1.5 to 2 g cm^{-2} . The polymers were coated by dropping 35 μL of each precursor solution onto the carbon-paper disc and photopolymerizing for 40 minutes. Typical weights of the polymers are 4 ~ 4.5 mg. After coating, the electrodes were dried in a vacuum oven overnight and transferred to a glove box filled with ultrapure Ar gas.

Estimation of the mesh size of the crosslinked network. A fully stretched polymer molecular mesh between two neighboring crosslinks was assumed and is considered to be one important characteristic of the network. A

ball-and-stick model clearly displays the connectivity of bonds and molecular geometries in ChemDraw® and was used to measure the distance between two adjacent crosslinkers. This model in ChemDraw® includes information about bond lengths, bond angles, and torsion angles, which are required for the calculation of the designated chain length.

Materials characterization. Attenuated total reflection Fourier transform infrared spectroscopy (ATR-FTIR) spectra were recorded by Thermo Scientific Nicolet 6700 FTIR equipped with a diamond ATR crystal. Spectra of the film samples were obtained between 4000 and 650 cm^{-1} for 64 scans with a resolution of 4 cm^{-1} . For the differential scanning calorimeter (DSC) test, samples were heated and monitored in the temperature range of -100~200 $^{\circ}\text{C}$ at 5 $^{\circ}\text{C min}^{-1}$ under a nitrogen gas atmosphere with a flow rate of 50 mL min^{-1} in a Mettler Toledo DSC 1. The glass transition temperature (T_g) of each sample was taken as the midpoint of a specific heat increment from the second heating run. X-ray photoelectron spectroscopy (XPS; Kratos Axis X-ray photoelectron spectrometer, monochromatic Al X-ray source (1486.6 eV)) was used to probe chemical interactions between polymers and lithium polysulfide species. The spectra were calibrated with the signals for C 1s at 284.8 eV and fitted with the Gaussian-Lorentzian peak profiles and Shirley-type background by CasaXPS software.

Electrochemical characterization. 2032-size coin half-cells with a Celgard 2500 separator were assembled and tested to characterize the electrodes. Lithium metal was used as counter and reference electrodes. 1 M lithium triflate (LiCF_3SO_3) in dimethoxyethane / 1,3-dioxolane (DME/DOL, 1/1 in volume) with 0.5 M LiNO_3 additive was used as an electrolyte for the test. The polymer-coated carbon disc was first soaked in the electrolyte for 6 hours before the cell assembly. The coin half cells were galvanostatically tested in a voltage range of 1.5 - 3.0 V vs. Li/Li^+ at 0.5C-rate where 1C-rate was defined as the current that can charge the theoretical capacity of sulfur, 1672 mAh g^{-1} , in an hour. For the *ex-situ* XPS and FTIR characterization, the cells were cycled twice at 0.2C and finally discharged to 1.5 V to form Li_2S . The disassembled electrodes were washed, soaked with DME, and transferred to the XPS chamber without air exposure.

Acknowledgement

JBG acknowledges support from the Welch Foundation (Grant number F-1066) and the Lawrence Berkeley National Laboratory BATT program (Project number 6998655). CJE acknowledges partial support from the Welch Foundation (Grant F-1709), 3M Nontenured Faculty Grant and DuPont Young Professor Award. KMM acknowledges support from the Department of Chemistry at Murray State University. JHC acknowledges partial financial support from LG Chem Graduate Research Fellowship and Graduate Dean's Prestigious Fellowship Supplement. The MTI Corporation is thanked for generous laboratory equipment donation.

References

- 1 A. Manthiram, Y. Fu, S.-H. Chung, C. Zu and Y.-S. Su, *Chem. Rev.*, 2014, **114**, 11751–11787.
- 2 Y. Yang, G. Zheng and Y. Cui, *Chem. Soc. Rev.*, 2013, **42**, 3018–3032.
- 3 L. F. Nazar, M. Cuisinier and Q. Pang, *MRS Bull.*, 2014, **39**, 436–442.
- 4 Q. Pang, D. Kundu, M. Cuisinier and L. F. Nazar, *Nat. Commun.*, 2014, **5**, 4759.
- 5 X. Tao, J. Wang, Z. Ying, Q. Cai, G. Zheng, Y. Gan, H. Huang, Y. Xia, C. Liang, W. Zhang and Y. Cui, *Nano Lett.*, 2014, **14**, 5288–5294.
- 6 C. J. Hart, M. Cuisinier, X. Liang, D. Kundu, A. Garsuch and L. F. Nazar, *Chem. Commun.*, 2015, **51**, 2308–2311.
- 7 Z. W. Seh, J. H. Yu, W. Li, P. Hsu, H. Wang and Y. Sun, *Nat. Commun.*, 2014, **5**, 5017.
- 8 M. Rosso, T. Gobron, C. Brissot, J.-N. Chazalviel and S. Lascaud, *J. Power Sources*, 2001, **97-98**, 804–806.
- 9 L. S. Cells, L. Ji, M. Rao, H. Zheng, L. Zhang, O. Y. Li and W. Duan, *J. Am. Chem. Soc.*, 2011, **133**, 18522–18525.
- 10 T. Lin, Y. Tang, Y. Wang, H. Bi, Z. Liu, F. Huang, X. Xie and M. Jiang, *Energy Environ. Sci.*, 2013, **6**, 1283.
- 11 A. B. Lowe, *Polym. Chem.*, 2010, **1**, 17–36.
- 12 K. Park, J. H. Cho, K. Shanmuganathan, J. Song, J. Peng, M. Gobet, S. Greenbaum, C. J. Ellison and J. B. Goodenough, *J. Power Sources*, 2014, **263**, 52–58.

- 13 K. Xu, *Chem. Rev.*, 2014, **114**, 11503–11618.
- 14 J. Zheng, D. Lv, M. Gu, C. Wang, J.-G. Zhang, J. Liu and J. Xiao, *J. Electrochem. Soc.*, 2013, **160**, A2288–A2292.
- 15 S. Urbonaite, T. Poux and P. Novák, *Adv. Energy Mater.*, 2015, 1500118.
- 16 J. Y. Koh, M.-S. Park, E. H. Kim, T. J. Kim, S. Kim, K. J. Kim, Y.-J. Kim and Y. Jung, *J. Electrochem. Soc.*, 2014, **161**, A2117–A2120.
- 17 X. Ji, K. T. Lee and L. F. Nazar, *Nat. Mater.*, 2009, **8**, 500–506.
- 18 Q. Wang, J. Zheng, E. Walter, H. Pan, D. Lv, P. Zuo, H. Chen, Z. D. Deng, B. Y. Liaw, X. Yu, X. Yang, J.-G. Zhang, J. Liu and J. Xiao, *J. Electrochem. Soc.*, 2015, **162**, A474–A478.
- 19 D. Aurbach, E. Pollak, R. Elazari, G. Salitra, C. S. Kelley and J. Affinito, *J. Electrochem. Soc.*, 2009, **156**, A694–A702.
- 20 Y. Diao, K. Xie, S. Xiong and X. Hong, *J. Electrochem. Soc.*, 2012, **159**, A1816–A1821.
- 21 A. Sarmigrahi, *J. Chem. Educ.*, 1986, **63**, 843–844.
- 22 A. B. Sannigrahi, T. Kar, B. Guha Niyogi, P. Hobza and P. V. R. Schleyer, *Chem. Rev.*, 1990, **90**, 1061–1076.
- 23 J. McMurry, *Organic chemistry*, 4th Ed. (Brooks/Cole publishing company, Pacific Grove, 1996).
- 24 J.-J. Chen, R. Yuan, J.-M. Feng, Q. Zhang, J.-X. Huang, G. Fu, M. Zheng, B. Ren and Q.-F. Dong, *Chem. Mater.*, 2015, **27**, 2048–2055.
- 25 Y. Yang, G. Zheng, S. Misra, J. Nelson, M. F. Toney and Y. Cui, *J. Am. Chem. Soc.*, 2012, **134**, 15387–15394.
- 26 M. A. Lowe, J. Gao and H. D. Abruña, *RSC Adv.*, 2014, **4**, 18347.
- 27 M. Cuisinier, C. Hart, M. Balasubramanian, A. Garsuch and L. F. Nazar, *Adv. Energy Mater.*, 2015, 1401801.
- 28 Y. Gorlin, A. Siebel, M. Piana, T. Huthwelker, H. Jha, G. Monsch, F. Kraus, H. a. Gasteiger and M. Tromp, *J. Electrochem. Soc.*, 2015, **162**, A1146–A1155.
- 29 A. Kawase, S. Shirai, Y. Yamoto, R. Arakawa and T. Takata, *Phys. Chem. Chem. Phys.*, 2014, **16**, 9344–50.
- 30 K. Mizoguchi, T. Higashihara and M. Ueda, *Macromolecules*, 2009, **42**, 3780–3787.

Table 1. Glass transition temperatures (T_g) of the cross-linked polymers (PETT-FC, PETT-EO, PETT-Ester, and PETT-Sulfone) measured by differential scanning calorimetry (DSC).

Materials	T_g (°C)
PETT-FC	6.3
PETT-EO	-30.9
PETT-Ester	-19.9
PETT-Sulfone	30.8

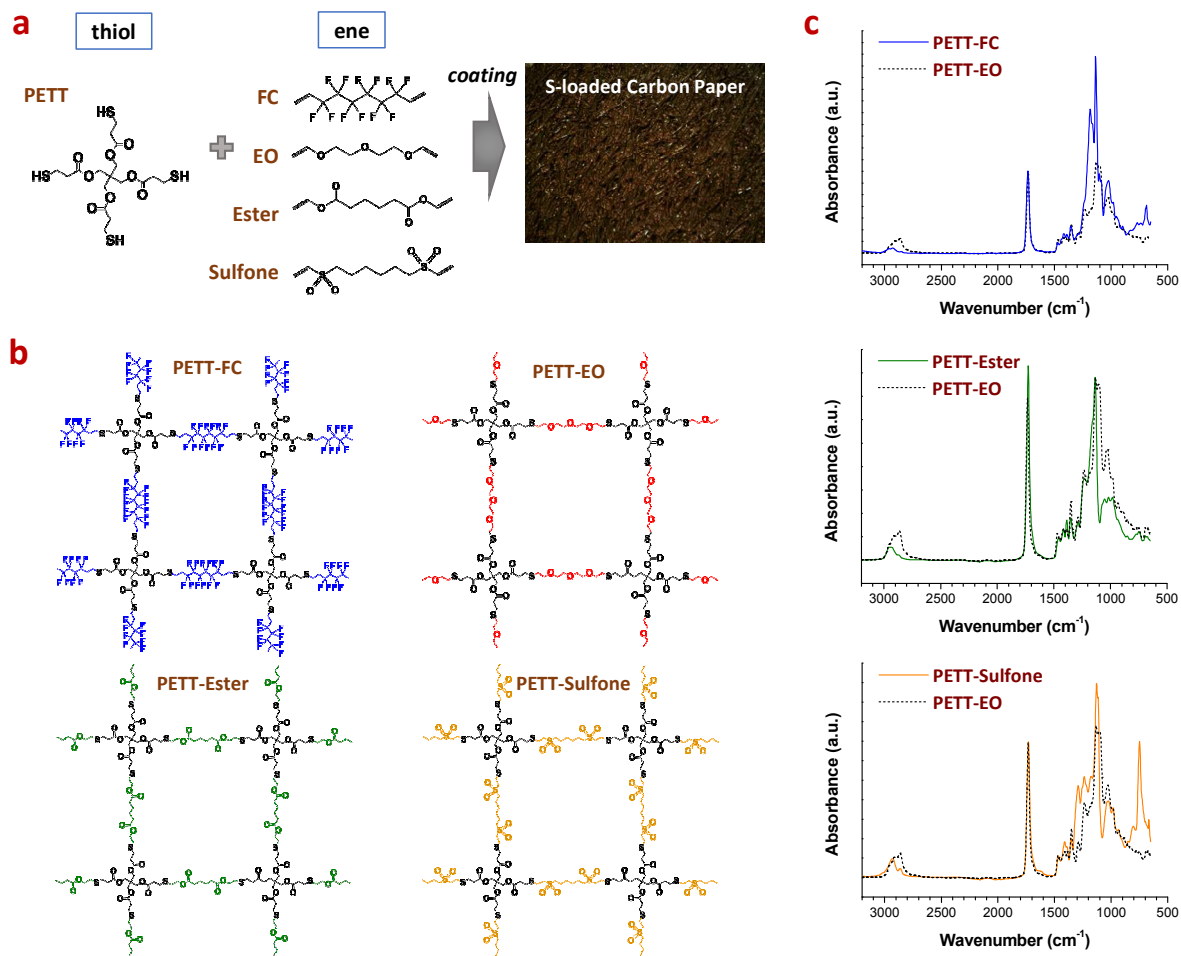


Figure 1. Synthesis of cross-linked polymers via thiol-ene chemistry. (a) Schematic representation of the thiol-ene reactions between a tetrathiol crosslinker and difunctional ene monomers to coat sulfur-loaded carbon paper electrodes. (b) Structure of PETT-FC, PETT-EO, PETT-Ester, and PETT-Sulfone and (c) their ATR-FTIR spectra.

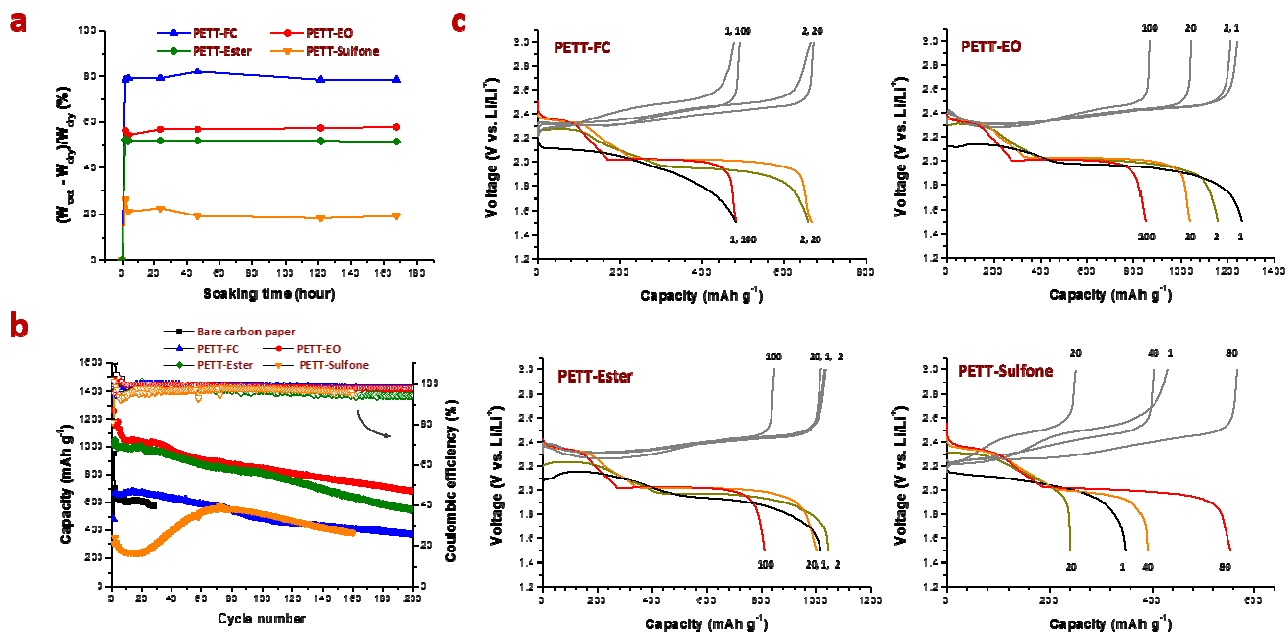


Figure 2. Electrochemical characterization of the polymer-coated sulfur electrodes. (a) Time-dependent electrolyte solvent (1:1 DME/DOL) uptake was measured and calculated according to the equation, $(W_{wet} - W_{dry})/W_{dry}$ where W_{dry} is the membrane weight before soaking and W_{wet} is the weight after liquid uptake. (b) Charge/discharge cycle performance and (c) voltage curves of PETF-FC, PETF-EO, PETF-Ester, and PETF-Sulfone electrodes measured between 1.5 and 3.0 V vs. Li/Li⁺ at 0.5C-rate.

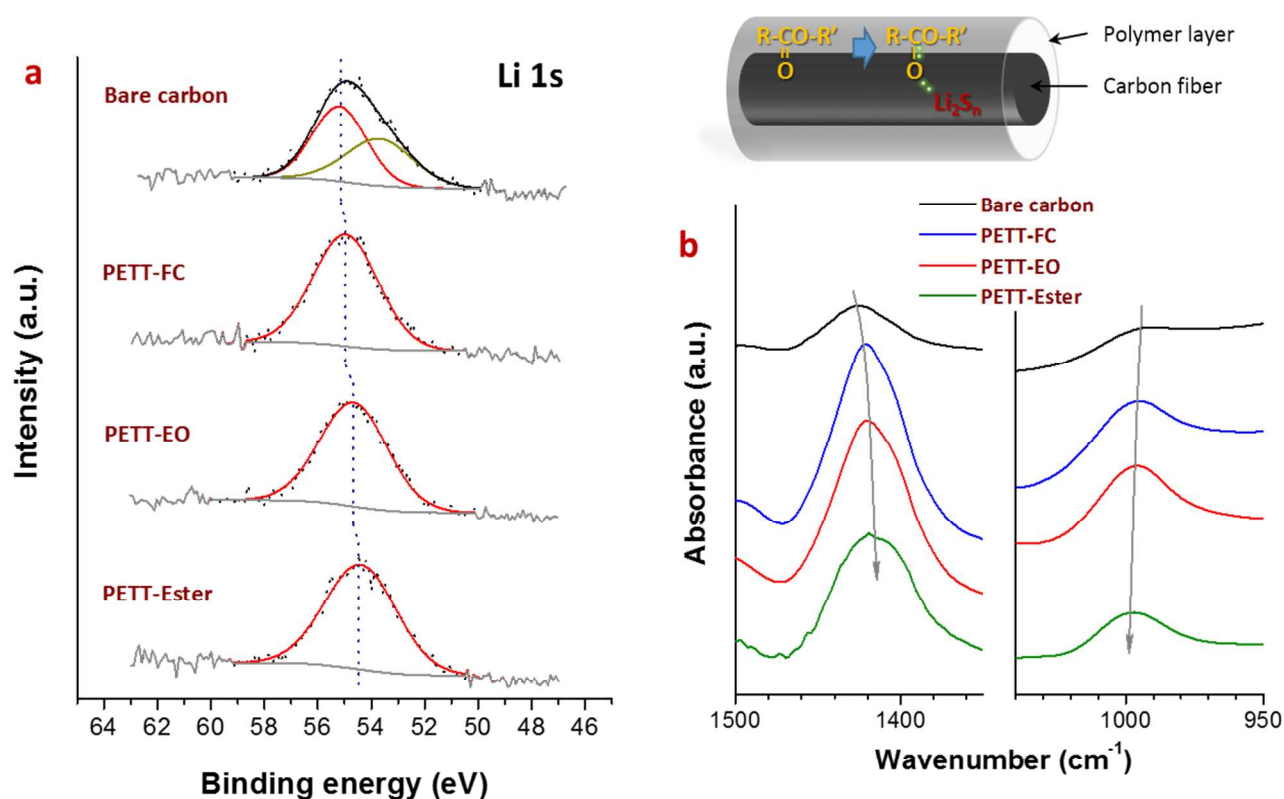


Figure 3. Chemical interactions between ester groups in the polymer backbone and lithium polysulfides. (a) Lithium 1s XPS and (b) ATR-FTIR spectra of the bare sulfur-loaded carbon, PETT-FC, PETT-EO, and PETT-Ester electrodes after discharging to 1.5 V. The electrodes were washed with DME and transferred to XPS chamber without any air exposure by using a transfer chamber. Schematic illustration proposes the lithium bond model between the ester group and lithium polysulfides.